

Slice imaging and velocity mapping using a single field

Vassilios Papadakis

Institute of Electronic Structure and Laser, Foundation for Research and Technology-Hellas, Voutes, 71110 Heraklion, Greece

Theofanis N. Kitsopoulos^{a)}

Institute of Electronic Structure and Laser, Foundation for Research and Technology-Hellas, Voutes, 71110 Heraklion, Greece and Department of Chemistry, University of Crete, Voutes, 71003 Heraklion, Greece

(Received 24 May 2006; accepted 19 June 2006; published online 2 August 2006)

In this study we demonstrate that it is possible to perform velocity mapping and slice imaging of charged particle products using a single field (two electrodes) improving on the multielectrode geometries of the past. The performance of this new geometry is competitive to the multielectrode ones, presently limited by detector “spot” resolution. For imaging both photoelectrons and photofragments a resolution of $\sim 1\%$ in velocity is achieved without further software manipulation such as event counting. The advantages of this new design are its ability to focus large volumes, its achromaticity (very little sensitivity on photofragment velocities), independence of the laser beam position in the field perpendicular to the extraction field, and compactness. Using this new design we have studied the photodissociation dynamics of pyrrole at 243 nm and show that internal conversion of electronically excited state molecules to the ground state is important even at such low excitation energies. © 2006 American Institute of Physics. [DOI: [10.1063/1.2222084](https://doi.org/10.1063/1.2222084)]

INTRODUCTION

Position sensitive detection of products has witnessed a tremendous amount of popularity in recent years.¹ In particular, imaging methods using optical relaying of the ion signals such that the spatial distribution of the particles can be captured using a digital camera have started to rival time of flight (TOF) applications. The original work of Chandler and Houston² has undergone several modifications that lead to this increase in popularity. In their seminal work, a beam of molecules was photodissociated using a polarized laser beam. The products were state selectively ionized using a resonant enhanced multiphoton ionization (REMPI) method, and the nascent ions were extracted using a homogeneous extraction field formed by a flat plate (repeller) and a flat fine grid (extractor). The principle of the method was very appealing but its limited resolution compared to TOF impeded its popularity. The main resolution problem was the physical dimensions of the molecular beam (~ 1 or 2 mm) which would be transferred over to the detector (typically 20 mm in radius) so at best the resolution achieved would be $\sim 10\%$ in velocity.

This limitation was overcome with the development of velocity mapping by Eppink and Parker in 1997.³ In this ingenious scheme the homogeneous field was replaced by an inhomogeneous field produced by three annular plates: the repeller, the extractor, and the ground electrode. By adjusting the relative voltage between the repeller and extractor, the field contours took on a shape that ensured a focusing of ion velocities “independent” of where they were produced in a plane perpendicular to the TOF axis (extraction field). This development elevated the imaging technique into great popularity replacing slowly but surely most TOF or magnetic

bottle machines for gas phase dynamics studies. The resolution has now improved by an order of magnitude down to 1% – 2% in velocity, making it competitive to TOF and additionally allows for enhanced angular distribution measurements. The only limitation remaining was the fact that these optically coupled imaging experiments relied on cylindrical symmetry of the measured distribution and on a noisy mathematical transform (the inverse Abel) to extract a “slice” through the three dimensional distribution.

The remedy to this cylindrical symmetry requirement was offered by the development of slice imaging in 2001 by Gebhardt *et al.*⁴ The basic principle is to introduce a temporal spread in the ion cloud along the TOF axis such as to allow a narrow detector gate to slice out the central part. There are presently two ways of doing this. The original design is of Gebhardt *et al.* where the extraction field is pulsed ON after a short delay following the photofragment ionization. The alternative method developed in 2003 concurrently by Townsend *et al.*⁵ and independently by Lin *et al.*⁶ relies on using a very weak acceleration field in the interaction region followed by strong acceleration. In both dc slicing approaches, the temporal spread is achieved in one electric field while a second field is used to achieve velocity mapping. In this study we introduce a new electrode design so as to that eliminate the need for the second field. In this new design a single repeller and a grounded extractor are sufficient to achieve both velocity mapping and slicing.

EXPERIMENT

Ion optics design

The basic principle behind velocity mapping is that by adjusting the voltages between two electrodes one achieves potential contours that are the optical analogy of a lens and will focus ion velocities onto the imaging plane of the detec-

^{a)}Electronic mail: theo@iesl.forth.gr

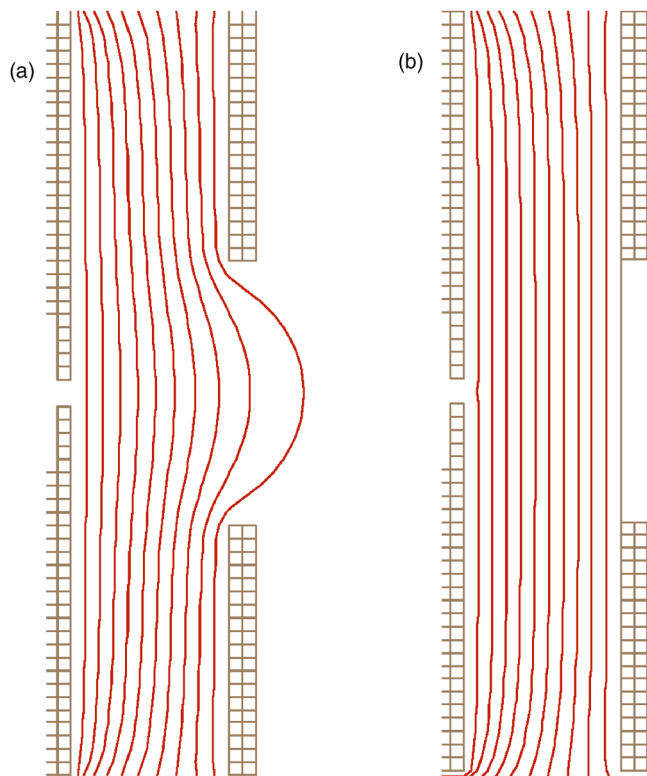


FIG. 1. (Color online) Simulations of potential contours created using the program SIMION for two parallel slits with and without grids.

tor. For comparison in Fig. 1 we consider two electrodes with 60 mm outer diameter, one with a 2 mm central aperture (repeller) and the second with a 20 mm aperture (grounded extractor). Applying any voltage to the extractor will form contours shaped like those shown in Fig. 1(a). In the optical analogy the contours resemble a plano-concave lens so that a ray (ion beam) propagating through this lens will diverge. If a flat grid is placed on the extractor, then the contours become flat and give rise to a homogeneous field as in the original design of Chandler and Houston. In this case no focusing is achieved but instead we have a geometric *spatial imaging* rather than *velocity imaging* (mapping).

In order to achieve focusing it is clear that we must

shape the contours to function as a plano-convex lens. To do so we introduce the ion optics design shown in Fig. 2. What we have done is to introduce a small step on both the electrode and the extractor electrodes. The exact dimensions for our design are given in Fig. 2 and are optimized for a TOF length of about 45 cm. Running ion trajectory simulations using SIMION 7.0 (Ref. 7) show that velocity mapping is achieved as indicated by the inserts in Fig. 2. The trajectories are calculated for ions of mass of 20 amu, kinetic energy of 5 eV, and a spatial extent perpendicular to the molecular beam of 4 mm. The focusing condition is met when the starting position along the TOF axis is at a specific distance from either the repeller or the extractor. Unlike existing velocity mapping and slicing methods where the focusing condition is met by adjusting the voltage on the second field (ion lens) in this new geometry the focusing is achieved by translating the laser position along the TOF axis.

The trajectories show that the focusing is maintained, independent of the repeller voltage, and also, unlike focusing using a second lens field, no or at least negligible amount of “chromatic” aberration is observed; more explicitly the focusing is independent of the initial center of mass velocity of the recoil particles. Simulations show that focusing of even 10 mm beams is possible down to better than 100 μm while for smaller beams (2 mm) it is predicted that a resolution better than 5 μm is possible.

If the grid is removed from the extractor the curvature of the contours on the side of the extractor dominates the focusing by the convex side of the repeller and focusing is not realized. However, if the size of the repeller rim is increased to 10 mm from 3 mm and the separation between repeller and extractor is increased to 35 mm from 22 mm, once again velocity mapping is possible as is shown in Fig. 2(b).

Slice imaging is achieved by delaying the extraction field with respect to laser ionization. Trajectory simulations using SIMION for both lens designs are shown in Fig. 3. We observe that both designs afford efficient temporal spreading along the TOF direction to allow for slicing. We do observe that when the grid is used, the temporal spread is substantially enhanced. The actual experimental performances of both designs are presented below.

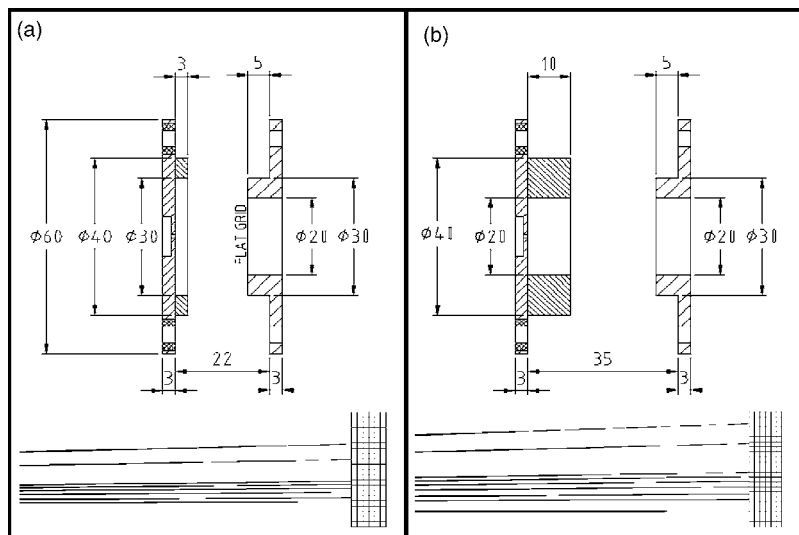


FIG. 2. Top: Detail design of the new ion optics used in the present experiment. Lower: Ion trajectories showing the velocity mapping capabilities of the respective ion optics. The interaction region consists of a 4 mm beam and fragments (20 amu) are ejected at 90° with respect to the TOF axis with energies of 5 eV.

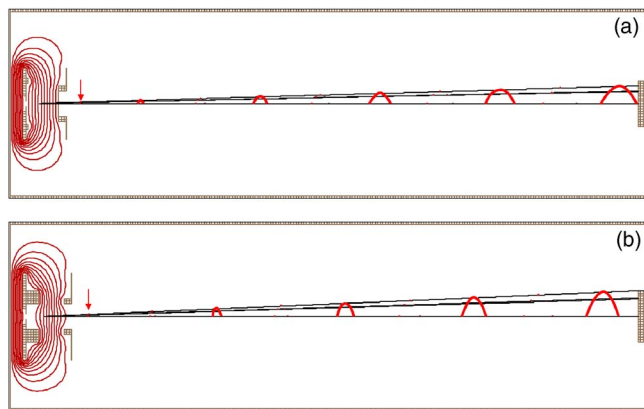


FIG. 3. (Color online) Ion trajectories showing the temporal evolution of the ion cloud following 300 ns delayed extraction (A) using grid and (B) without grids. The time step is 500 ns for each trajectory.

Imaging

The details of the experiment have been described elsewhere.⁴ Two major changes have been made, the first concerning the ion optics described in the previous section and the second regarding the camera imaging system. The new camera is an IEEE1394 (Firewire) digital 12 bit camera SONY XCD-710, 1/3 in. charge coupled device (CCD), 1024×768 resolution, controlled using National Instruments (NI) LABVIEW 7.1 and IMAQ Vision software. In the present software design any IEEE1394 camera with NI IMAQ drivers available can be used in a plug and play fashion using this software. Adjustments of the camera gain, on chip integration time, option trigger or asynchronous mode, averaging, background subtraction, real time line profiling, display of both real time and averaged image, control of delay boxes, and expandability are also possible.

To test the performance of the new ion optics experiments were performed on the following systems: (a) imaging photoelectrons from the (2+1) REMPI of Xe at 252.5 nm and (b) imaging of H atoms following the photolysis of HBr and pyrrole at 243.2 nm.

RESULTS AND DISCUSSION

Velocity mapping

Shown in Fig. 4 are the photoelectron speed distributions obtained from photoelectron images using appropriate image processing obtained for the various ion optics geometries of Fig. 2, and also using the geometry of Fig. 2(b) but with no molecular beam. The results clearly indicate that there is essentially no degradation in the resolution of the experiment for the quality of grids (40 lines/mm) used in our experiments. What is most impressive is that the resolution degradation in the absence of the molecular beam, using only background gas where we estimate that the interaction volume must be greater than 10 mm (we use 300 mm focal length lens for the REMPI). The particle focusing is sensitive to the laser position displacement along the TOF axis. In our setup, the position of the interaction region is controlled by moving the optical lens using a standard translation stage and the focusing condition is met within 1 full turn ($500 \mu\text{m}$) of this stage. A major feature of this single field focusing irre-

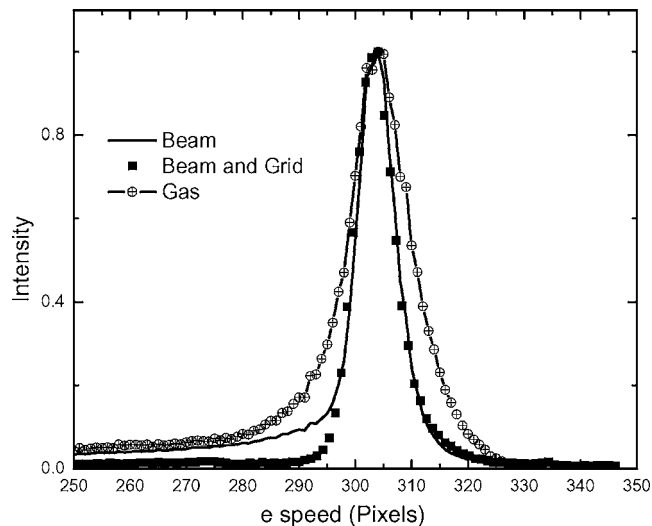


FIG. 4. Photoelectron speed distribution following the (2+1) REMPI of Xe at 252.5 nm. Results are shown for geometries using a 2 mm molecular beam and ion optics with and without grids. Also shown is the speed distribution obtained using the gridless ion optics but with no molecular beam (only background Xe gas).

spective of gridless or with grid design is that the position of the images is not displaced when the laser is displaced perpendicular to the imaging plane, even in the case of the gas cell experiment. This is another testament to the very efficient velocity focusing (mapping) of this design.

Slice imaging

To test the slicing performance of the new design we first performed experiments on the H-atom imaging following the photolysis of HBr at 243.2 nm.⁸ Slice images using a grid are obtained by delaying the extraction field 50 ns after the ionization, and are shown in Fig. 5(a). Line profile at 0° with respect to the laser polarization and speed distributions are shown in Fig. 5(b). At this wavelength (2+1) REMPI of H atoms is also possible and as reported elsewhere, a recoiling of the H^+ ions from the photoelectron causes a splitting in the H-atom speed distribution. This splitting is clearly resolved, and from the doublet separation we determine that the velocity resolution of this design is just as good as conventional velocity mapping designs, i.e., on the order of 1% or better. Using centroiding and other deconvolution software this “raw” resolution can be improved further.^{9–12}

In spite of the SIMION predictions [Fig. 3(b)], compared to the geometry using the grid, the gridless geometry did not perform satisfactorily in slicing mode in spite of its excellent velocity mapping results. More detail experiments will be performed to understand why this occurred and to improve the performance.

Photodissociation of pyrrole at 243 nm

Pyrrole has been studied by several research groups both theoretically and experimentally.^{13–21} It is used as a model system in order to understand better the photochemical behavior of small DNA bases. The photodissociation dynamics of pyrrole at 243 nm have been studied both by Wei *et al.*¹⁴ and Cronin *et al.*¹⁵ Both experiments observed loss of the H

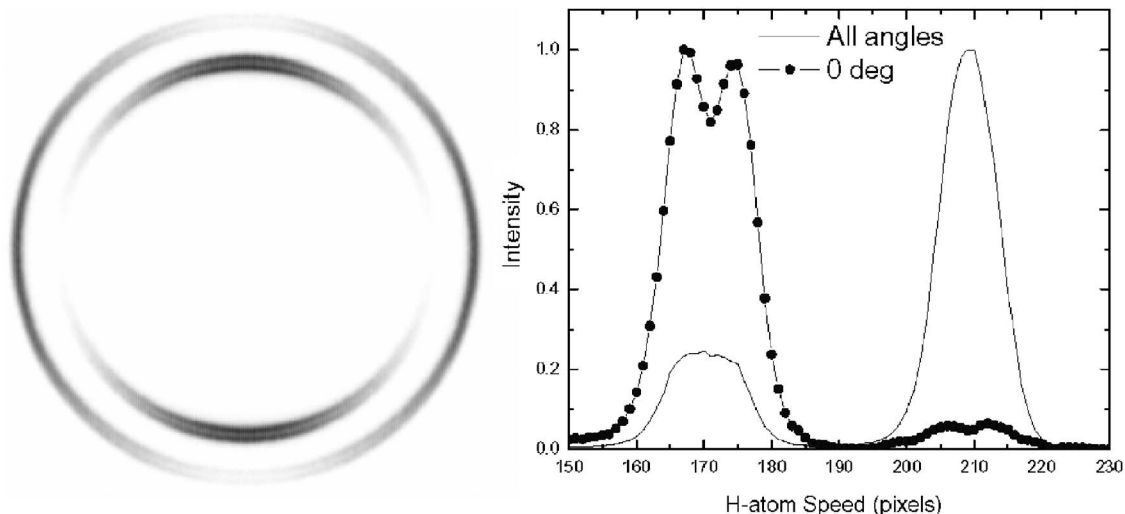


FIG. 5. Slice image of H atoms from the photolysis of HBr at 243.2 nm. H atoms are detected using (2+1) REMPI at 243.2 nm. The speed distribution obtained by integrating the slice image over all angles is shown as well as intensity profile at 0° with respect to the vertical axis. The laser polarization is vertical.

atom that is bonded to the nitrogen atom. The velocity distribution observed was bimodal consisting of an intense fast channel and a weaker slower channel. In the experiments of Schnieder *et al.* the unsurpassed velocity resolution offered by H atom the Rydberg tagging²² method, allowed the vibrational structure to be observed for the fast channel. However, their signal to noise ratio at the low velocities did not allow the definite assignment of the low velocity channel. On the other hand the 4π collection efficiency of the imaging method used by Wei *et al.* was able to measure both channels with satisfactory signal to noise ratio. However, because of the inherent resolution limitation (as mentioned above) of detecting H atom using (2+1) REMPI at 243 nm, no vibrational structure was observed.

Because H atoms are very fast it is usually necessary to scan the Doppler profile of the resonant transition in order to detect all velocities of the H-atom fragments. In our experiment the probe laser consists of a Nd:YAG (yttrium aluminum garnet) pumping an (optical parametric oscillator) (OPO) system (Spectra Physics 730D10). We observe that when the Nd:YAG is not seeded, the bandwidth of the OPO output broadens enough such that we are able to measure the “entire” velocity profile of the fragments without scanning the laser. As described elsewhere, we measure slice images obtained in the X and Z geometries (laser polarization perpendicular and parallel to the TOF axis, respectively), which are shown in Fig. 6. The kinetic energy distribution of the H atoms is also shown in Fig. 6 and is calibrated using the $D_0(\text{N-H})=32\,850\text{ cm}^{-1}$ reported by Schnieder *et al.* Our distribution as in the work of Wei *et al.* is bimodal, and the ratios of the slow and fast peaks are very similar. The shape of the slower peaks differs slightly but follows qualitatively very closely the shape of the slow H-atom distributions observed in the photolysis of pyrrole at lower wavelengths ($\lambda < 220\text{ nm}$). This would suggest that the mechanism of production of slow H atoms and consequently internally hot pyrrolyl radical even at the long wavelength of 243 nm used here is probably the same. This mechanism has been sug-

gested to involve internal conversion from the excited 1A_2 state to the ground state through a conical intersection. It has been observed that increasing the kinetic energy increases the propensity of the slow channel.

The Z image is used for calibration, correcting any errors due to detector inhomogeneities and velocity biasing because the probe laser is not scanned. Shown in Fig. 7 are the normalized angular distributions obtained from the X-slice image. Anisotropy parameters found for the fast and slow channels are $\beta_{\text{fast}}=-0.33\pm 0.005$ and $\beta_{\text{slow}}=-0.008\pm 0.002$. The value for β_{fast} is in excellent agreement with the previous

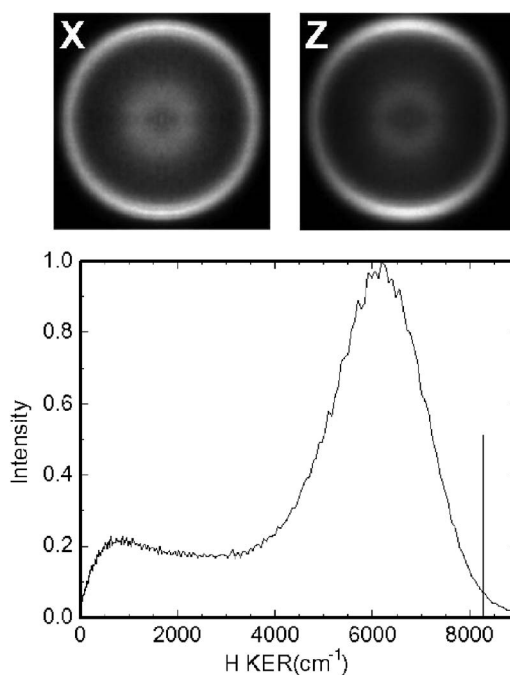


FIG. 6. Top: Slice images of H atoms following the photolysis of pyrrole at 243.2 nm. The laser polarization is parallel (Z) and perpendicular (X) to the TOF axis. Lower: Kinetic energy distribution (KER) obtained from the slice images. The vertical line indicates the origin (maximum allowed kinetic energy).

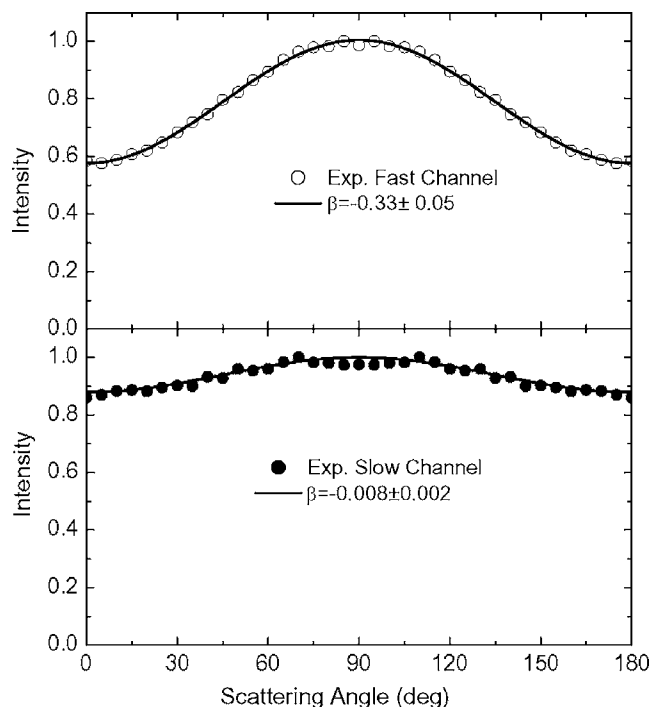


FIG. 7. Angular distribution for the fast and slow channels obtained from the slice images of Fig. 6.

measurement of Wei *et al.* while β_{slow} at 243 nm is reported here for the first time. At 243 nm it is believed that pyrrole is excited from the ground S_0 state directly to the 1A_2 state and the molecule dissociates. The negative β value observed for the fast channel is consistent with this explanation; however, the β value does not approach the limiting value of -1 . This deviation can be attributed to lifetime broadening, i.e., non-prompt dissociation or possibly contribution of another pathway, namely, a parallel transition to the 2^1A_1 state. Comparison of the β values between the fast and slow channels results in a reduction in the anisotropy parameter by exactly a factor of 4. This is what one would expect in the very long lifetime limit.

We have demonstrated that it is possible to perform velocity mapping and slice imaging using a single acceleration field. We have applied this new geometry both to photoelectron velocity mapping and photofragment slice imaging. Using this method to study the dynamics of pyrrole at 243 nm we have shown that internal conversion of the excited state

molecules to the ground state is important even at these low excitation energies. Extension of the method presented here to full collision experiments is planned.

ACKNOWLEDGMENTS

This work is supported by the transfer of knowledge program SOUTHERN DYNAMICS MTKD-CT-2004-014306. This work was performed at the Ultraviolet Laser Facility operating at IESL-FORTH and has been supported in part by the European Commission through the Research Infrastructures activity of FP6 ("Laserlab-Europe" RII3-CT-2003-506350). The authors thank the graduate program Applied Molecular Spectroscopy (EPEAEK).

- ¹ *Imaging in Molecular Dynamics*, edited by B. J. Whitaker (Cambridge University Press, Cambridge, 2003).
- ² D. W. Chandler and P. L. Houston, *J. Chem. Phys.* **87**, 1445 (1987).
- ³ A. T. J. B. Eppink and D. H. Parker, *Rev. Sci. Instrum.* **68**, 3477 (1997).
- ⁴ C. R. Gebhardt, T. P. Rakitzis, P. C. Samartzis, V. Ladopoulos, and T. N. Kitsopoulos, *Rev. Sci. Instrum.* **72**, 3848 (2001).
- ⁵ D. Townsend, M. P. Minitti, and A. G. Suits, *Rev. Sci. Instrum.* **74**, 2530 (2003).
- ⁶ J. J. Lin, J. Zhou, W. Shiu, and K. Liu, *Rev. Sci. Instrum.* **74**, 2495 (2003).
- ⁷ www.simiom.com
- ⁸ R. L. Toomes, P. C. Samartzis, T. P. Rakitzis, and T. N. Kitsopoulos, *Chem. Phys.* **301**, 209 (2004).
- ⁹ B. Y. Chang, R. C. Hoetzlein, J. A. Mueller, J. D. Geiser, and P. L. Houston, *Rev. Sci. Instrum.* **69**, 1665 (1998).
- ¹⁰ W. Li, S. D. Chambreau, S. A. Lahankar, and A. G. Suit, *Rev. Sci. Instrum.* **76**, 063106 (2005).
- ¹¹ M. L. Lipciuc, J. B. Buijs, and M. H. M. Janssen, *Phys. Chem. Chem. Phys.* **8**, 216 (2006).
- ¹² F. Renth, J. Riedel, and F. Temps, *Phys. Chem. Chem. Phys.* **77**, 033103 (2006).
- ¹³ D. A. Blank, S. W. North, and Y. T. Lee, *Chem. Phys.* **35**, 187 (1994).
- ¹⁴ J. Wei, A. Kuezmman, J. Riedel, F. Renth, and F. Temps, *Phys. Chem. Chem. Phys.* **5**, 315 (2003).
- ¹⁵ B. Cronin, M. G. D. Nix, R. H. Qadiri, and M. N. R. Ashfold, *Phys. Chem. Chem. Phys.* **6**, 5031 (2004).
- ¹⁶ A. L. Sobolewski and W. Domcke, *Chem. Phys.* **259**, 181 (2000).
- ¹⁷ M. H. Palmer, I. C. Walker, and M. F. Guest, *Chem. Phys.* **238**, 179 (1998).
- ¹⁸ L. Serrano-Andres, M. Merchan, I. Nebot-Gil, B. O. Roos, and M. Fulscher, *J. Am. Chem. Soc.* **115**, 6184 (1993).
- ¹⁹ B. O. Roos, P. A. Malmqvist, V. Molina, L. Serrano-Andres, and M. Merchan, *J. Chem. Phys.* **116**, 7526 (2002).
- ²⁰ A. L. Sobolewski, W. Domcke, C. Dedonder-Lardeux, and C. Jouver, *Phys. Chem. Chem. Phys.* **4**, 1093 (2002).
- ²¹ J. Wan, J. Meller, M. Hada, M. Ehara, and H. Nakatsuji, *J. Chem. Phys.* **113**, 7853 (2002).
- ²² L. Schnieder, W. Meier, K. H. Welge, M. N. R. Ashfold, and C. M. Western, *J. Chem. Phys.* **92**, 7027 (1990).